EAN 2024 62th annual conference on experimental stress analysis

Validation of Simulation of the Temperature Field of a Part during Selective Laser Melting Procedure

R. Skácelík [1,a] , M. Španiel [1]

[1] *Department of Mechanics, Biomechanics and Mechatronics, Faculty of Mechanical Engineering, Czech Technical University in Prague, Technická 4, 160 00 Prague 6, Czech Republic*

[a] *radek.skacelik@fs.cvut.cz*

Abstract: The heat that is supplied to the printed part during the selective melting procedure must be dissipated so that the part does not overheat. The procedure fulfilling this requirement can be effectively designed using validated numerical simulations. The measurement of the temperature field on the top layer of the part using a thermocamera placed in the area of printing is the main topic of the contribution. The measured temperature field is compared with one obtained from simulation employing the finite element method. The comparison provides us with the validation of both the finite element model and computational procedure which are described in the paper as well.

Keywords: 3D printing; thermal camera; finale element method; recoating; selective laser melting.

1 Introduction

Selective laser melting is one of the additive technologies based on melting metal powder. The principle consists of consecutive application of thin layers of metal powder in a workspace that is locally melted at the sites of the printed part. This creates a solid occupying the entire geometry of the printed part while the rest of the workspace remains filled with powder [1]. The processing parameters, i.e. laser input power, scanning speed and slit pitch, have a significant effect on the heat supplied and, consequently on the temperature of the part. This heat is dissipated through the part to the platform. The part is subjected to dimensional changes due to the thermal expansion of the material. This reduces the quality and the consistency of the thickness of the new layers applied. In extreme cases, this can result in the closure of the gap between the part and the coating device, causing print failure. Such accidents reduce the efficiency of the entire process and therefore it is an effort to be able to predict them before the actual printing of the part takes place.

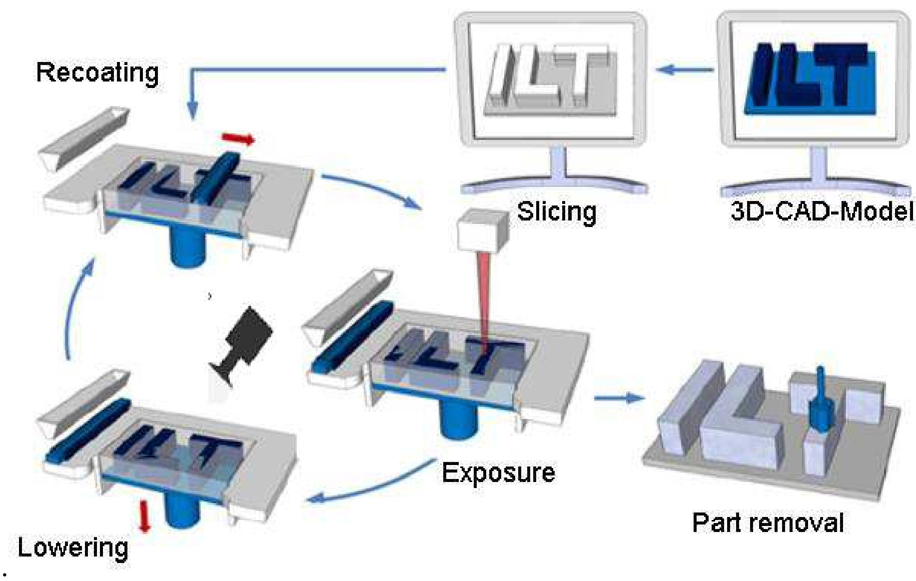

Fig. 1: Printing scheme with the location of the measurements in the printing cycle indicated. [3]

The motivation of this work is to validate a numerical model to describe the distribution of temperature fields inside a printed part. Due to the limited possibilities to verify the temperature distribution of the part, a thermal camera was used to measure the residual temperature of the sample (Fig. 1, lowering section). This was used to measure the temperature of the surface before the coating was swiped. These temperatures are monitored to observe the history and trends of temperature evolution as the geometry of the part changes.

2 Methods

2.1 Printer Configuration

In this work, the TRIUMF 1000 printer was used for the measurements. This printer has a circular print base with a diameter of 100 mm and the height of the print area is approximately 150 mm. A thermal camera (Fig. 2) was installed in the press compartment, and during the creation of the new layer, the camera lens was covered by a servo-controlled aperture. The servo was controlled depending on the position of the coating and the printing time. The measurements were performed with a FLIR Lepton 3.5 thermal imaging camera whose compact dimensions allow it to be placed close to the printing area. The pixel density of the measurement is about 1 pixel per square millimeter. The raw data was transferred from the thermal camera directly to the computer where the data was processed and averaged. The sample was placed in the middle of the platform. The measurement point was chosen in the middle of the sample and the temperature values were averaged using the surrounding pixel values.

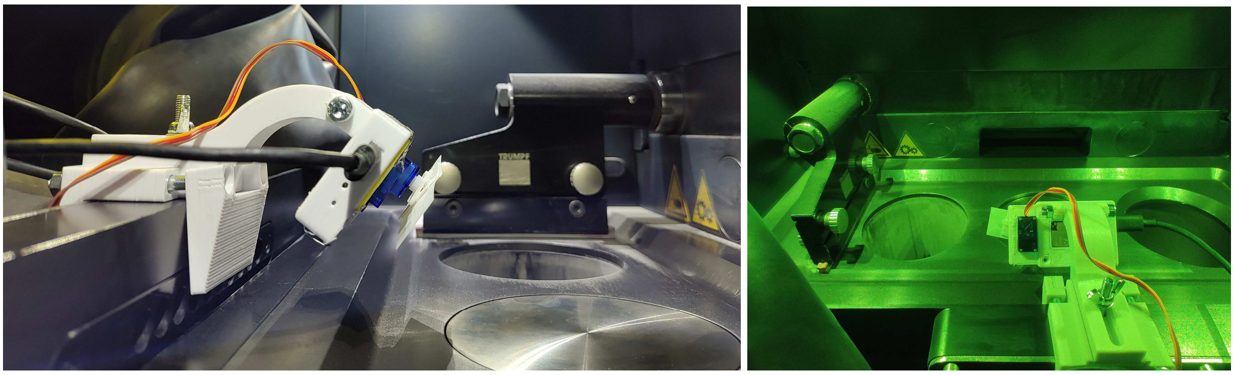

Fig. 2: Printer area configuration.

2.2 Calibration of the Thermal Camera

The thermal camera was calibrated using a modified method described in [1]. The model was not heated directly in the printer but was heated in an annealing furnace. Subsequently, the sample was fitted with a thermocouple. The thermocouple was placed in a groove printed directly into the sample so that it had the largest possible heat transfer surface near the top of the cube (Fig. 3). After the thermocouple had equilibrated the temperature with the sample, the emissivity coefficient of the surface of the top of the cube was adjusted according to this temperature value so that the temperature value from the thermocouple matched that from the thermal imager. The sample was then scanned throughout the cooling period to determine the deviation between the thermocouple and thermal camera values.

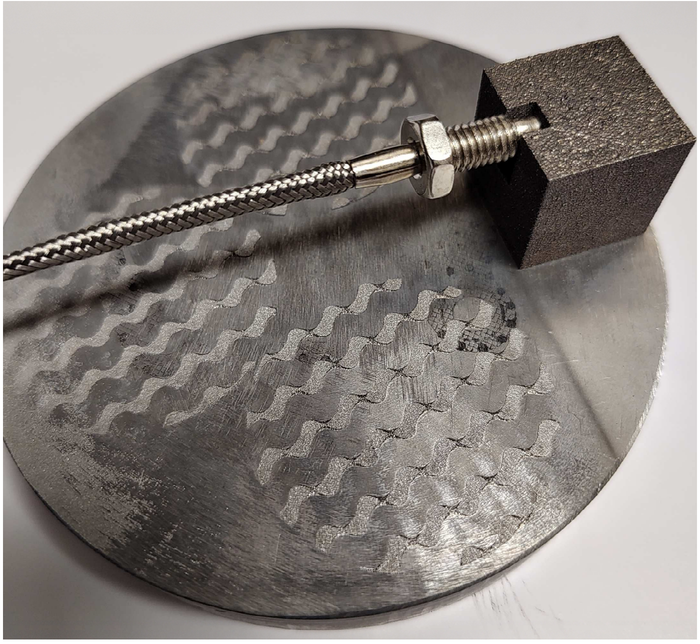

Fig. 3: Sample on the platform with thermocouple.

2.3 Experimental Sample and Build Plan

Measurements were taken on a sample (Fig. 4) that has a circular base and then widended at a 45-degree angle. The rotationally symmetric body was chosen to eliminate as much as possible the effect of asymmetric cooling due to heat transfer from the body to the powder. MS-1 tool steel was chosen as the specimen material. The laser power is 250 W, the scanning speed is 1000 mm/s, the grating is 0.1 mm and the layer thickness is 0.04 mm. The coater waited 4 s after each layer was applied before the next layer was applied. It took 3 s to apply a new layer of powder. The frequency of the laser return to a single point is shown in Fig. 5. In this case, the amplitude correlates with the area of each layer of the body. This is due to the location of a single sample on the platform. The sample is deliberately chosen so that the total amount of heat delivered to the sample increases as a function of the area of the top layer.

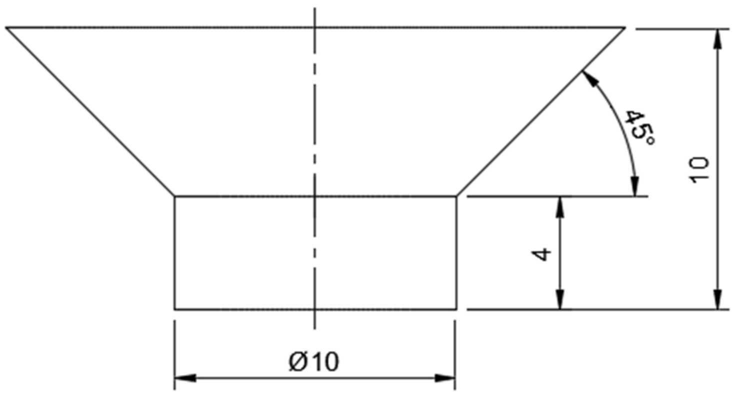

Fig. 4: Geometry of the sample.

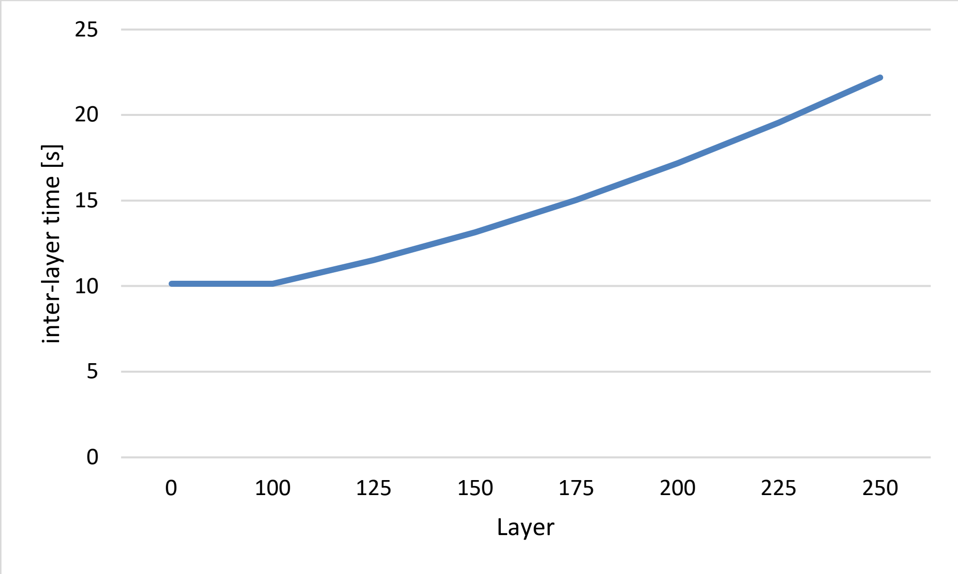

Fig 5: Internal layer time of the printed sample.

2.4 Numerical Simulation

The same parts as in the experiment were also used to calculate the temperature fields by simulation of the printing procedure using the finite element method. The mesh density and intensity of the temperature source were adjusted so there would be a match with the experiment. A modified Oofem and Code-Aster solver code was used for the calculation. The sample model was meshed using a voxel-type mesh (Fig. 6). This mesh includes a portion of the base.

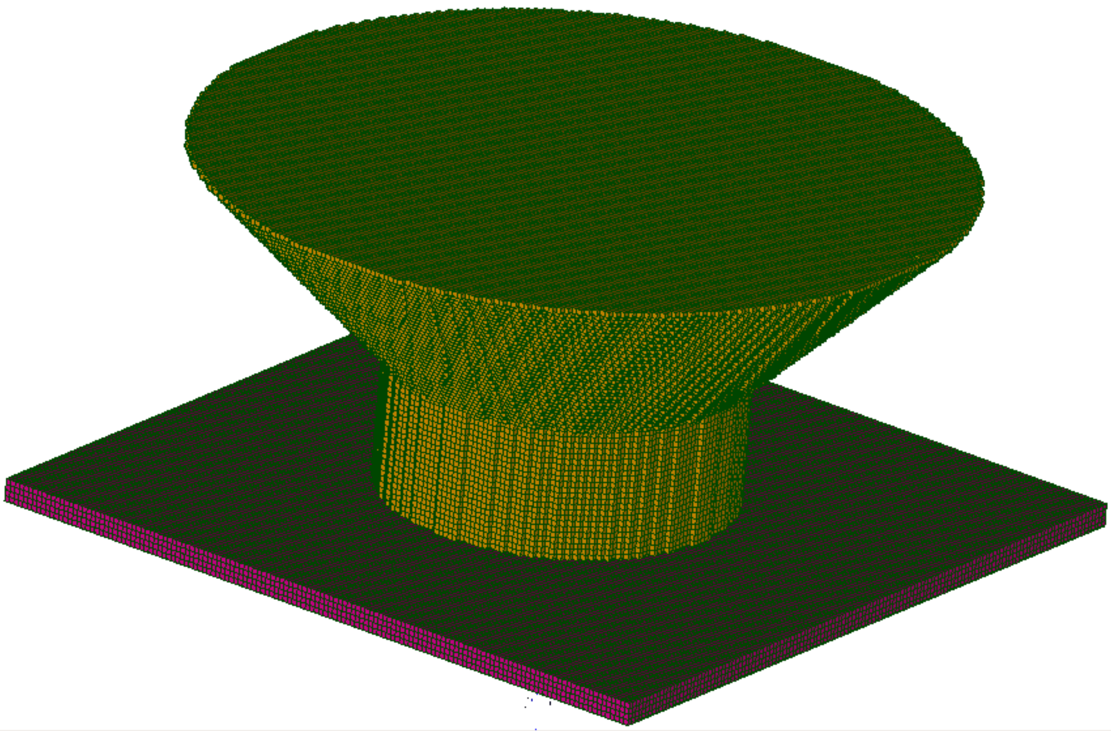

Fig. 6: Mesh of the sample (brown) and base (purple).

The simulation was performed using the flash heating method. This method Is based on heating the entire top layer at once. The hot top layer serves as a loading boundary condition from which the heat is then distributed to the entire model. In this type of simulation, the temperature of the added layer is set as the solidification temperature of the molten metal. The cooling time of the part before the next layer is applied is determined from the internal layer time (ILT) (Fig. 5). In the case where multiple layers (super layer thickness SLT) are applied simultaneously, the cooling time is increased in proportion to the number of layers merged.

3 Results and Discussion

By comparing the temperature of the sample measured by the thermocouple and the thermocamera, the emissivity coefficient of the printed part surface was found. This coefficient was determined to be 0.35 for the tool steel used.

By measuring the temperature history of the sample, it was found that the part heats up with increasing top layer area (Fig. 7), despite the fact that the ILT increases with increasing area (Fig. 5).

The finite element method was used to predict the temperature history of the sample. Several different element sizes (SLT) were used and the result was compared with the temperature waveform of the experimental sample. Sufficient agreement with the experiment was achieved for elements with a thickness of 3 real layers (Fig. 7).

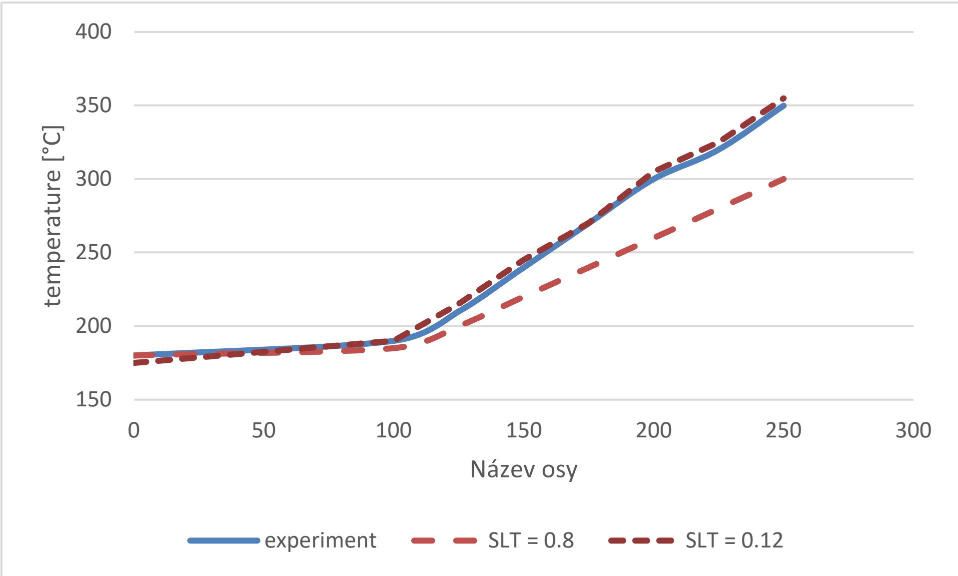

Fig. 7: Results of simulation and measurements.

4 Conclusion

Calibration and temperature measurements were made using a thermal imager during printing at the moment before the new layer was applied. These values were used to validate the results of the finite element simulation.

References

[1] T. DebRoy, H.L. Wei, J.S. Zuback, T. Mukherjee, J.W. Elmer, J.O. Milewski, A.M. Beese, A. Wilson-Heid, A. De, W. Zhang, Additive manufacturing of metallic components – process, structure and properties, Progress in Material Science 92 (2018) 112–224, https://doi.org/10.1016/j.pmatsci.2017.10.001.

[2] M. Montazeri, P. Rao, Sensor-based build condition monitoring in laser powder bed fusion additive manufacturing process using a spectral graph theoretic approach, Journal of Manufacturing Science and Engineering 140 (9) (2018) MANU-18-1023, https://doi.org/10.1115/1.4040264.

[3] US Research Nanomaterial, “Strain less steel powder” [online], available at: http://www.us-nano.com/inc/sdetail/14838. [Zugriff am 15 September 2017].